

High-cycle fatigue life prediction for Pb-free BGA under random vibration loading

Da Yu^a, Abdullah Al-Yafawi^a, Tung T. Nguyen^a, Seungbae Park^{a,c,*}, Soonwan Chung^b

^a Department of Mechanical Engineering, State University of New York at Binghamton, P.O. Box 6000, Binghamton, NY 13902, USA

^b Samsung Electronics, Ltd., Republic of Korea

^c Department of Advanced Technology Fusion, Konkuk University, Seoul, Republic of Korea

ARTICLE INFO

Article history:

Received 12 July 2010

Received in revised form 1 September 2010

Accepted 5 October 2010

Available online 10 November 2010

ABSTRACT

This paper develops an assessment methodology based on vibration tests and finite element analysis (FEA) to predict the fatigue life of electronic components under random vibration loading. A specially designed PCB with ball grid array (BGA) packages attached was mounted to the electro-dynamic shaker and was subjected to different vibration excitations at the supports. An event detector monitored the resistance of the daisy chained circuits and recorded the failure time of the electronic components. In addition accelerometers and dynamic signal analyzer were utilized to record the time-history data of both the shaker input and the PCB's response.

The finite element based fatigue life prediction approach consists of two steps: The first step aims at characterizing fatigue properties of the Pb-free solder joint (SAC305/SAC405) by generating the *S-N* (stress-life) curve. A sinusoidal vibration over a limited frequency band centered at the test vehicle's 1st natural frequency was applied and the time to failure was recorded. The resulting stress was obtained from the FE model through harmonic analysis in ANSYS. Spectrum analysis specified for random vibration, as the second step, was performed numerically in ANSYS to obtain the response power spectral density (PSD) of the critical solder joint. The volume averaged Von Mises stress PSD was calculated from the FEA results and then was transformed into time-history data through inverse Fourier transform. The rainflow cycle counting was used to estimate cumulative damages of the critical solder joint. The calculated fatigue life based on the rainflow cycle counting results, the *S-N* curve, and the modified Miner's rule agreed with actual testing results.

© 2010 Elsevier Ltd. All rights reserved.

1. Introduction

Failure causes in electronic components can be classified as shock/impact-induced, vibration-induced, and thermal-induced failures. Since the thermal loading appears to be the major cause of electronic component failures, most of research work has focused on the failure mechanisms and fatigue life prediction models under thermal loading, while relatively limited work considered vibration loading. In the field-use conditions, and during their manufacturing process, shipping and service life, however, electronic components are exposed to different vibration loadings. Especially for avionic and automotive electronic systems which experience a great amount of vibration during their service life, the vibration-induced failure is one of the most important reliability issues.

Most electronic systems used in vibration environments are subjected to random vibration loading instead of ordinary harmonic excitations. However, a large portion of research on high-

cycle fatigue is only concerned with predicting the fatigue life of electronic components exposed to a sinusoidal vibration. Chen et al. [1] combined the vibration failure test, FEA, and theoretical formulation for the calculation of the electronic component's fatigue life under sinusoidal vibration loading. Che et al. [2] employed vibration fatigue test and analysis methodology for flip chip solder joint fatigue life assessment. Perkins and Sitaraman [3] used linear sweep vibration test to characterize the fatigue failure for ceramic column grid array (CCGA). Yang et al. [4] characterized the dynamic properties of a plastic ball grid array (PBGA) assembly with a sweep sine excitation.

In the area of random vibration fatigue, Pitarresi et al. [5–7] considered the modeling techniques of circuit cards subjected to vibration loading. They investigated the response of surface mount lead/solder and predicted its fatigue life subjected to random excitation. Wong et al. [8] developed an experimentally validated vibration fatigue damage model for a plastic ball grid array (PBGA) solder joint assembly. Effective strains were calculated and combined with the three-band techniques to predict solder joint survivability. Mei-Ling Wu [9] developed a rapid assessment methodology that can determine the solder joint fatigue life of ball grid array (BGA) and chip scale packages (CSP) un-

* Corresponding author. Address: Department of Advanced Technology Fusion, Konkuk University, Seoul, Republic of Korea. Tel.: +1 607 777 3415; fax: +1 607 777 4620.

E-mail address: sbpark@binghamton.edu (S. Park).

der vibration loading. Li [10] presented a methodology of failure analysis of electronic components under automotive vibration environment.

In contrast to the previous research, in this work the lead-free solder's $S-N$ curve was generated from sinusoidal vibration tests and used for the fatigue life prediction of electronic components. Zhou et al. [11] has proposed the $S-N$ models for SAC305 and Sn37Pb and Chin et al. [12] produced a fatigue characterization curve – the E–N curve for the BGA component, however, for the first time, the high-cycle fatigue durability for SAC alloys with different Ag content (SAC305/SAC405) was thoroughly investigated. In addition, an assessment methodology based on vibration tests and finite element analysis (FEA) to predict the high-cycle fatigue life of electronic components under random vibration loading was developed.

In the random vibration simulation, the volume-averaged stress response PSD was obtained and used in estimating the cumulative damage of solder joint, which is more realistic than the widely used three-band method [13]. Steinberg's three-band method is a simplified method for the prediction of random vibration fatigue life, which assumes that the response stress follows normal distribution. Under this assumption, the response stress within the $1-\sigma$ level, $2-\sigma$ level, $3-\sigma$ level results in 68.3%, 95.4%, and 99.7% of the time, respectively, where the σ level stresses can be obtained from ANSYS. Since the σ level stresses are statistical quantities, the three-band method provides quick but less accurate fatigue life estimation, as shown in the previous work [14], than the methodology applied in this work.

2. Vibration tests and analysis

2.1. Test vehicle and experimental set-ups

Two specially designed BGA packages with built-in daisy chain circuit assembled on a PCB is used in the vibration tests. The components and the corresponding daisy chain circuits are shown in Fig. 1. The BGA component, $12\text{ mm} \times 12\text{ mm}$, is mounted with 0.3 mm diameter lead-free solder balls in 0.5 mm pitch. The PCB is made of FR4 with 100 mm in length, 50 mm in width, and has a thickness of 0.6 mm . Lead-free solder $96.5\text{Sn}-3.0\text{Ag}-0.5\text{Cu}$ (SAC305) and $95.5\text{Sn}-4.0\text{Ag}-0.5\text{Cu}$ (SAC405) were used in those test vehicles. Lowering Ag content in SAC alloys reduces the elastic modulus as shown in Table 1. This paper presents the detailed fatigue life prediction procedure of SAC305 solder balls and briefly shows the $S-N$ curve and high-cycle fatigue life prediction results of SAC405.

To perform vibration tests, the PCB assembly is mounted on the shaker with aluminum standoffs screwed to four corner screw holes as shown in Fig. 2. Accelerometers and dynamic signal analyzer were utilized to record the time-history data of both the shaker input and the PCB's response, and to obtain the transmissibility function of the test vehicle.

An event detector was used to monitor the resistance of the daisy chain circuits continuously throughout the test and to record the failure time. Once a crack is initiated in one of the solder joints

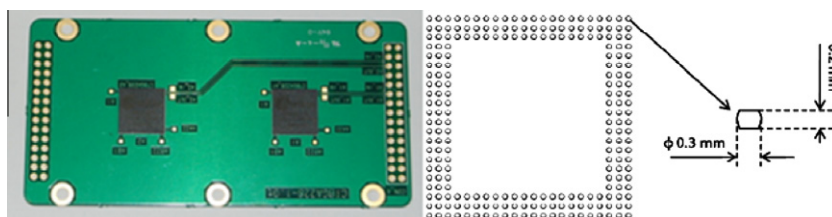


Fig. 1. Details of test vehicle.

Table 1
Material properties used in the FEA model.

Materials	Young's modulus, (GPa)	Poisson's ratio	Density, (kg/m^3)
PCB	25.0	0.28	3400
Substrate	22.0	0.28	2000
Solder ball (SAC405) [18]	53.3	0.35	7440
Solder ball (SAC305) [18]	51.0	0.36	7400
Molding compound	20.0	0.30	1890

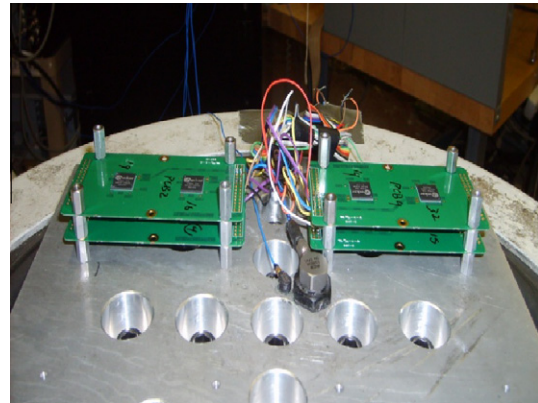


Fig. 2. Experiment set-up of vibration tests.

during the vibration test, the resistance of the daisy chain will increase. According to the IPC standard [15], the failure criterion is defined as an increase of the daisy chain resistance by 20% of its initial value consecutively six times.

The high-cycle fatigue life prediction procedure is shown in Fig. 3. A 3D FEA model was first verified through natural frequencies, mode shapes and transmissibility function. The volume-averaged stress was then obtained from harmonic analysis in the FEA model. Together with the number of fatigue cycle results from sinusoidal test, $S-N$ curve was generated. Random vibration was performed both numerically and experimentally. Volume averaged PSD was extracted from FEA model to produce the time-history data. Rainflow cycle counting and modified Miner's rule were applied to estimate cumulative damage of the critical solder joint.

3. Finite element analysis for vibration test

3.1. Finite element model

Since the solder balls were too small to directly measure the stresses, FEA was used instead to obtain the stresses for the fatigue estimation of the electronic components. In this study, the FEA model as presented in Fig. 4 was constructed with the commercial software ANSYS 11.

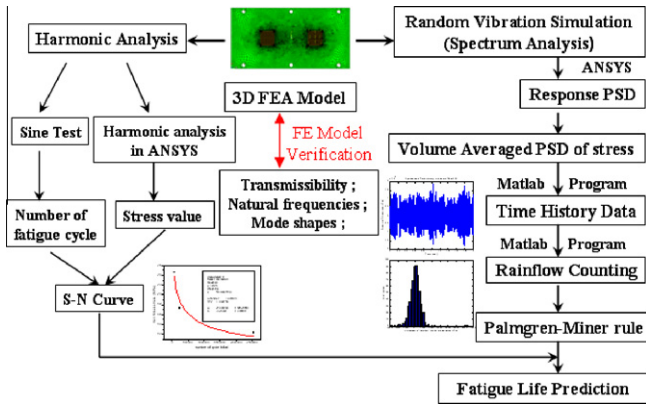


Fig. 3. High-cycle fatigue life prediction procedure.

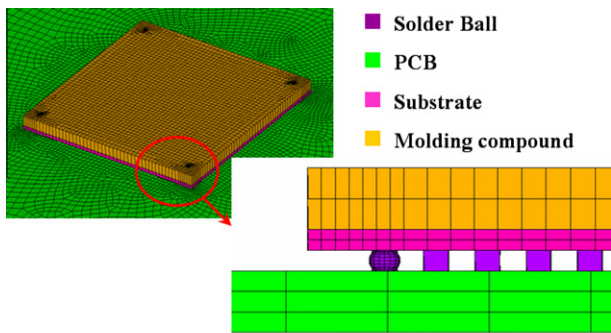


Fig. 4. 3D finite element model of the BGA package.

According to the reliability assessment work of the PBGA assembly [16,4], the vibration fatigue failure always occurred at the corner solder balls of the package under the vibration loading. Therefore, solder balls at the four corners of the BGA were modeled in detail while equivalent cubes were used to represent all other solder balls in this model. Unlike the submodeling technique, which requires post-processing, this 3D finite element full model saves a large amount of post-processing time while retains a reasonable accuracy.

Solid element (SOLID45) was used to model all components in this model including the PCB. Since boundary conditions should represent those used in the vibration test, all nodes at the screw holes were fixed in all degrees of freedom.

In high-cycle fatigue studies, the deflections, stresses, and strains are estimated with the assumption of elastic response [17]. Therefore, linear elastic material properties were applied in this numerical model as listed in Table 1.

3.2. Modal analysis

Natural frequencies and mode shapes are important parameters that characterize the dynamic responses of test vehicle during vibration test. Modal analysis was performed experimentally to determine these parameters and to validate the FEA model. Fig. 5 shows the test set-up of the modal analysis where the grid was marked on the test vehicle with an accelerometer attached to one of the grid points and an instrumented hammer was used to excite all points with random input following fixed response approach. The accelerometer and the instrumented hammer were connected to a multi-channel FFT analyzer which collected both input and output responses and calculated the frequency response

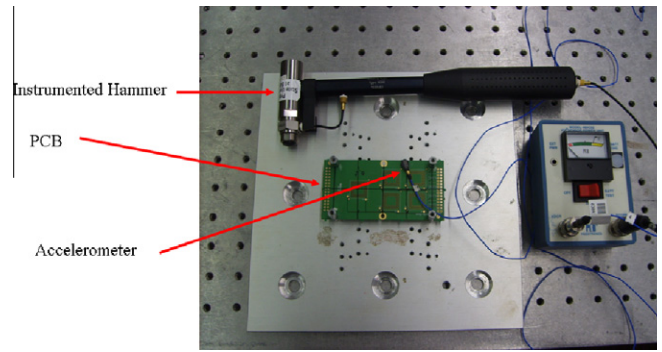


Fig. 5. Experiment set-up of modal analysis.

Table 2

Comparison of natural frequencies and mode shapes from FEA and modal test for SAC305.

	First mode	Second mode	Third mode
FEA (Hz)	281	519	768
Experiment (Hz)	282	521	757
FEA			
Experiment			

function (FRF). Star software was finally used to generate the mode shapes from all grid points.

Table 2 shows the comparison of first three natural frequencies and mode shapes as obtained from the modal analysis experimentally and numerically. A good agreement between FEA and experimental result is shown as the error percentages of FEA results relative to those of modal test results are all within 2%.

3.3. Frequency-scanning test

The frequency-scanning test was performed as a white noise input acceleration PSD applied to the shaker over a frequency range between 100 and 1000 Hz. Two accelerometers were used to characterize the system (Fig. 6); one accelerometer was placed on the shaker fixture to measure the input acceleration to the system, G_{in} , and the second accelerometer was placed on top of the PCB to measure the output acceleration, G_{out} .

For better correlation of the FE model with vibration test results, damping needs to be applied in this FE model. The damping ratio was determined through frequency-scanning test by half-power bandwidth method (as shown in following equation) for the lightly damped structure.

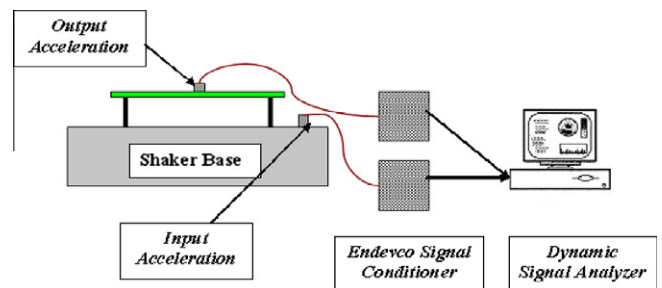


Fig. 6. Schematic of shaker test system.

$$\zeta = \frac{\Delta f}{2f_n} \quad (1)$$

where Δf is the bandwidth of the half-power points. These half-power points are frequencies where the response is $1/\sqrt{2}$ or 0.707 of its peak value.

Fig. 7 shows the output acceleration power spectral density (G_{out}) when test vehicle was swept from 100 to 1000 Hz with an input acceleration PSD of $0.001 \text{ g}^2/\text{Hz}$. The results from 260 Hz to 300 Hz are presented for the sake of clarity, as the output acceleration PSD beyond this range is roughly constant at $0.001 \text{ g}^2/\text{Hz}$. Using $f_n = 281 \text{ Hz}$ and $\Delta f = 3 \text{ Hz}$, the damping ratio ζ was found to be 0.005.

The transmissibility can be estimated by:

$$T = \frac{G_{out}}{G_{in}} \quad (2)$$

Fig. 8 indicates the transmissibility is well correlated with the incorporation of damping in this FEA. Transmissibility function verification together with modal analysis verification provides sufficient confidence on the current FE model for the further random vibration fatigue prediction.

3.4. Harmonic analysis

After the 1st natural frequency was determined from previous tests, the sinusoidal test was performed in order to characterize fatigue properties of the solder joint material by generating its $S-N$ curve. In the sinusoidal test, the sweep frequency range was 5% around natural frequency of 282 Hz, which is from 265 Hz to 295 Hz. Different vibration tests were conducted by varying the constant G-level (5G, 7G, 8.5G (except for SAC405), and 10G input excitation). The failure time was measured during vibration tests for each G-level excitation.

Failure analysis of the time to failure from sinusoidal tests was conducted using a two-parameter Weibull distribution model as shown in Figs. 9a and b

$$F(t) = 1 - \exp \left[- \left(\frac{t}{\eta} \right)^\beta \right] \quad (3)$$

where $F(t)$ is the cumulative failure distribution function, η is referred as characteristic life and is the number of failure cycles at which 63.2% of the devices failed, β is the shape parameter.

It is clearly shown in Table 3 that the time to failure decreases as the input excitation G-level increases. Also, as expected, SAC305

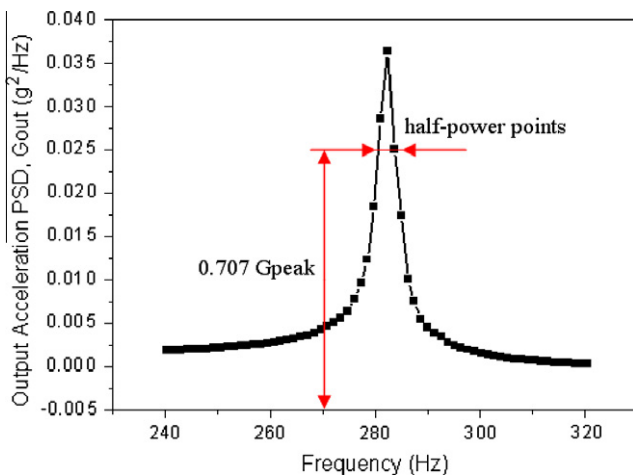


Fig. 7. Vibration test result to determine the damping ratio.

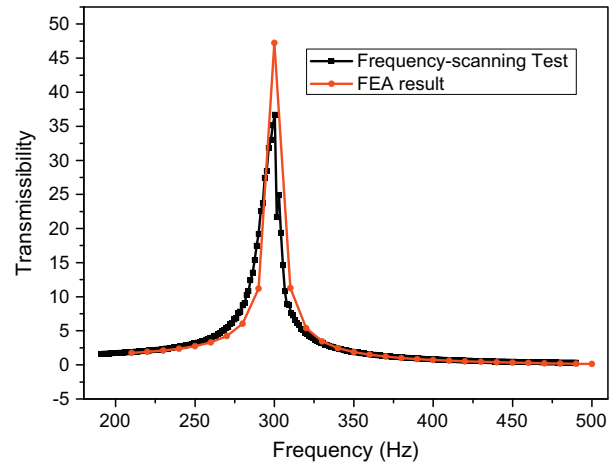


Fig. 8. Comparison of transmissibility obtained from FEA with experiment.

is found to outperform SAC405 with higher fracture resistance under vibration conditions, since low-Ag alloys are found to have both high bulk compliance and high plastic energy dissipation ability [18,19].

3.5. Stress analysis and $S-N$ curve generation

The equivalent stress, known as the Von Mises stress, is more appropriate to be used in this fatigue life prediction model. The amplitude of other stress components is much lower except the peeling stress along the solder ball axis. As the mesh density around the solder/PCB interface affect its stress distribution, the volume-average method is applied over a thin layer of elements at solder/PCB interface to compensate for this effect. The volume averaged Von Mises stress over this layer can be calculated by:

$$\sigma_{avg} = \frac{\sum \sigma \cdot V}{\sum V} \quad (4)$$

According to Fig. 10, which shows the Von Mises stress distributions of solder balls, the outmost corner solder ball was observed to have stress concentration along the solder/PCB interface. The volume-averaged stress over thin layer at this critical solder joint was calculated and used for the $S-N$ curve.

3.6. Fatigue cycle determination

The sinusoidal vibration test was conducted at a constant logarithmic sweep rate (1 octave/min). For the logarithmic sweep [20]:

$$\log f = At + B \quad (5)$$

where A and B are constants to determine the sweep rate. For example, the sweeping from 5 Hz to 200 Hz for 10 min ($f = 5 \text{ Hz}$ at $t = 0$, and $f = 200 \text{ Hz}$ at $t = 600$) results in the values of the constants $A = 0.00267$ and $B = 0.7$. From Eq. (5), we have

$$dt = \frac{1}{Af \ln 10} df \quad (6)$$

The actual number of cycles for each frequency interval then can be estimated by:

$$\Delta n = f \Delta t = \frac{1}{A \ln 10} \Delta f \quad (7)$$

Most of the damage accumulated during a sweep through the resonant point of a structural assembly will occur near the peak response point. A convenient reference is the half-power points, used extensively by electrical engineers to characterize resonant peaks

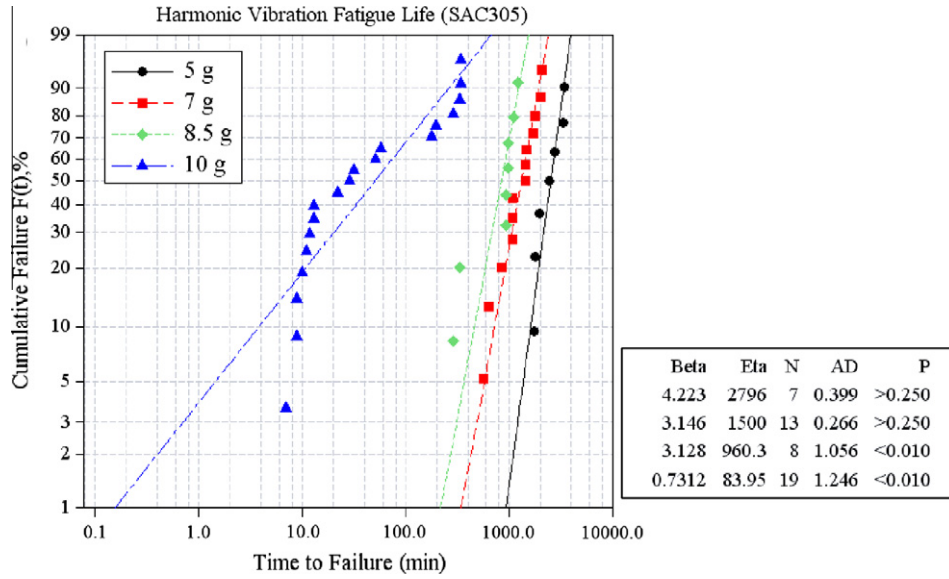


Fig. 9a. Weibull distribution of time to failure for different G-level sinusoidal tests (SAC305).

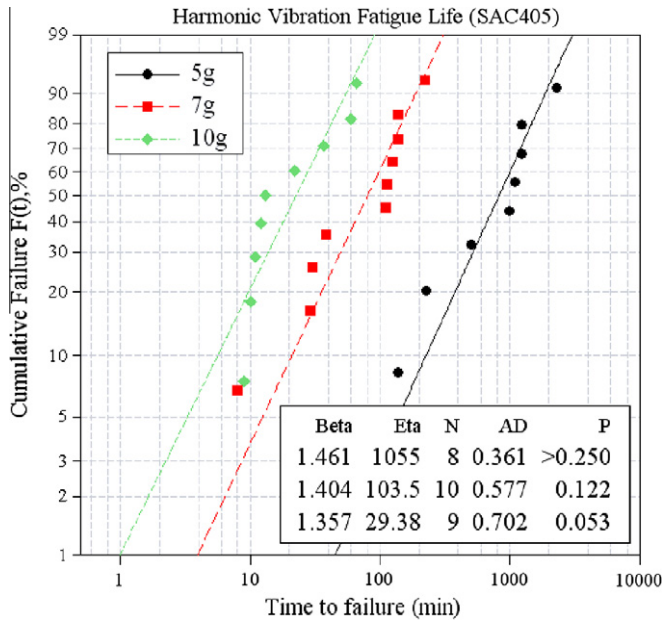


Fig. 9b. Weibull distribution of time to failure for different G-level sinusoidal tests (SAC405).

Table 3
Characteristic life for sinusoidal tests.

Characteristic life	5 g	7 g	8.5 g	10 g
SAC305 (min)	2796	1500	960.3	83.95
SAC405 (min)	1055	103.5	N/A	29.38

in electronic circuits [13]. Therefore, number of fatigue cycles under sinusoidal vibration was calculated based on frequency band between half-power points.

Fig. 11 shows the Von Mises stress amplitude response of critical solder ball from the FE harmonic analysis.

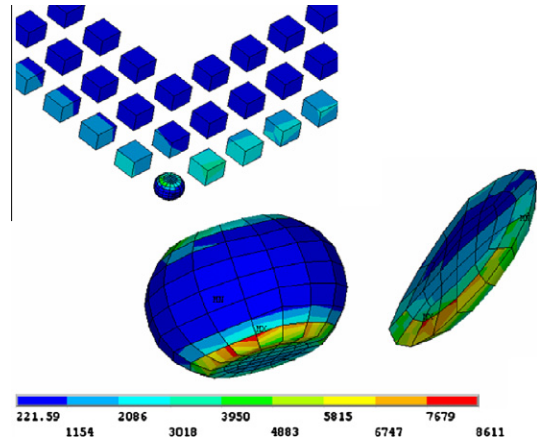


Fig. 10. Equivalent stress distributions on solder balls.

The frequency range between the half-power points is 5 Hz as indicated in Fig. 11. The fatigue cycle can be determined from the following equation.

$$\Delta n = f \Delta t = \frac{1}{A \ln 10} \Delta f = \frac{5}{A \ln 10} \tag{8}$$

The expected fatigue life of a solder ball typically exceeds 10,000 cycles under vibration condition. The failure is mainly attributed to the stress based high-cycle fatigue as characterized by Basquin power law relation:

$$\sigma_a = \sigma'_f (2N_f)^b \tag{9}$$

where σ_a is stress amplitude, σ'_f is fatigue strength coefficient, b is fatigue strength exponent, $2N_f$ is reversals to failure.

With the calculated Von Mises stress (S) from FEA and fatigue cycles (N) from vibration tests, the constants σ'_f and b were determined to be 64.8 MPa and -0.1443 (Fig. 12a), respectively, for SAC305, and 152.2 MPa and -0.2079 (Fig. 12b), respectively, for SAC405 through linear regression analysis. It is worth noting that the value of b traditionally used for 63Sn37Pb is -0.25 [21]. Yao et al. [22] also determined those material constant for 63Sn37Pb

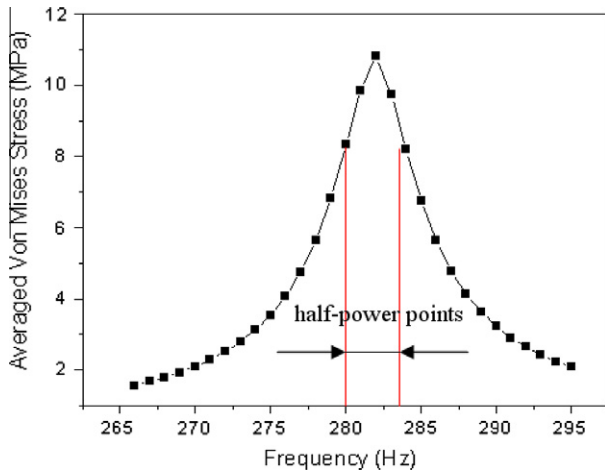


Fig. 11. Von Mises stress response of critical solder ball under sinusoidal test.

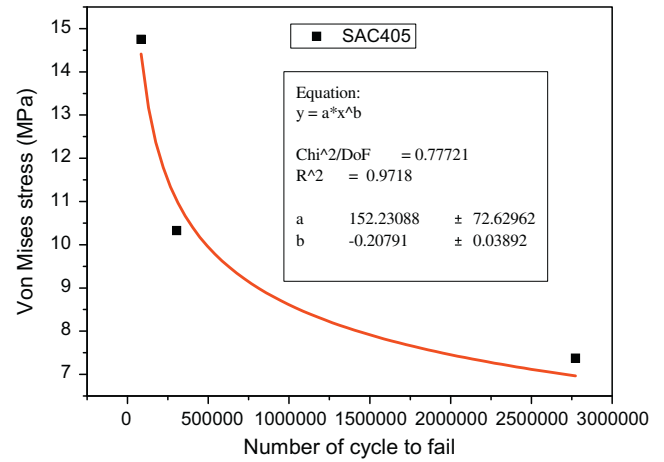


Fig. 12b. S-N curve for SAC405.

solder, which are 177.15 MPa and -0.2427 , respectively. The eutectic solder's S-N curves as provided by Manson [23] and Steinberg [13] are 66.3 MPa, -0.12 and 109.6 MPa, -0.10 , respectively.

3.7. Random vibration tests

Electro-dynamic shaker (LDS V830) was operated to run random vibration fatigue tests. Uniaxial loading was applied to the test vehicles in its out-of-plane direction. The power spectral density is the most commonly used function to describe a random vibration in the frequency domain. The white noise PSD with different acceleration amplitude ($0.15 \text{ g}^2/\text{Hz}$, $0.25 \text{ g}^2/\text{Hz}$) is set as input PSD over a frequency range between 40 and 1000 Hz. The frequency range was selected based on a study conducted by NASA to analyze the in-flight vibration environment, where the PSD of the measured vibration showed peaks at 65 Hz, 85 Hz, 105 Hz, 130 Hz, 200 Hz, and 500 Hz [24].

The volume averaged PSD of the Von Mises stress (Fig. 13) over a thin layer of elements at solder/PCB interface in critical solder joint, which is the same thin layer in harmonic analysis, is determined through Eq. (10) after running spectrum analysis in ANSYS to predict its high-cycle fatigue.

$$S_{ave}(w_i) = \left(\frac{\sum_{j=1}^{N_v} \sqrt{S_j(w_i)} * V_j}{\sum_j V_j} \right)^2 \tag{10}$$

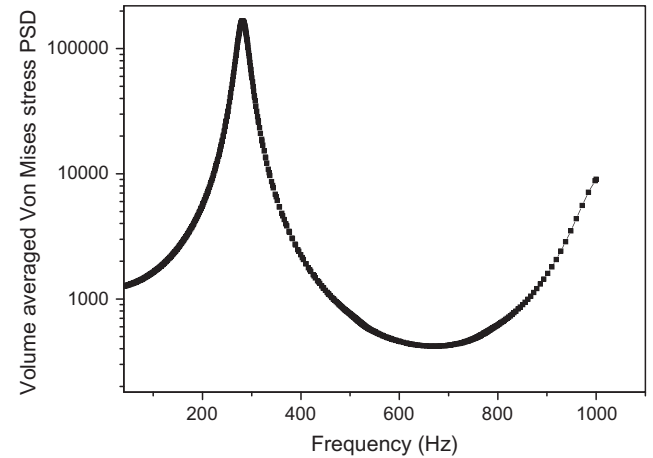


Fig. 13. The volume averaged PSD of the Von Mises stress at critical solder joint.

where V_j is the volume of each element, S_j is the Von Mises stress PSD of each element obtained from the spectrum analysis.

This volume averaged power spectrum is then transformed into time-history data (Fig. 14) using the IFFT method. A unit sample of 2 s time-history data is generated. The total record can then be reproduced by repeating the unit sample over the test time. The generated time history should be statistically equivalent to the original PSD. To verify the accuracy of the generated time series data corresponding to the given power spectrum, the area under the PSD curve was compared with the mean square value of the time series data, which theoretically should be identical. Results show that both values are close to each other (the area under PSD curve = $7.899\text{e}6$, Fig. 13, the mean square value of time series data = $7.896\text{e}6$, Fig. 14).

The rainflow counting method is applied in the analysis of fatigue data in order to reduce the spectrum of varying stress into sets of simple stress reversals for different amplitudes. It allows the application of Palmgren–Miner's rule to assess the fatigue life of a structure subject to complex loading. This rule states that the incremental damage due to each cycle can be simply added to estimate the fatigue life. The damage due to one cycle may be expressed as [17]

$$\Delta D_i = \frac{1}{N_i} = \frac{1}{C} \left[\frac{(1/2)\Delta S_i}{1 - S_{mi}/S_u} \right]^b \tag{11}$$

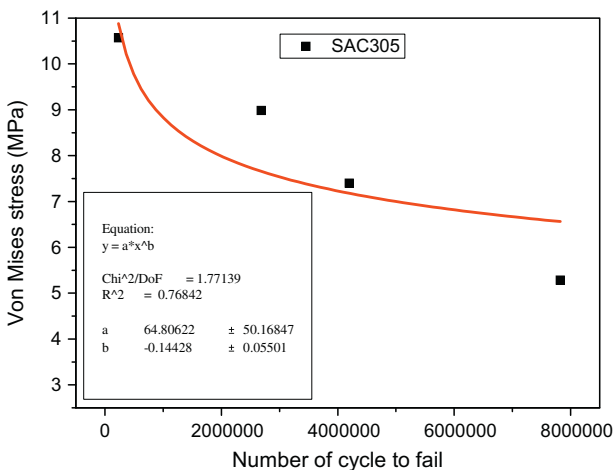


Fig. 12a. S-N curve for SAC305.

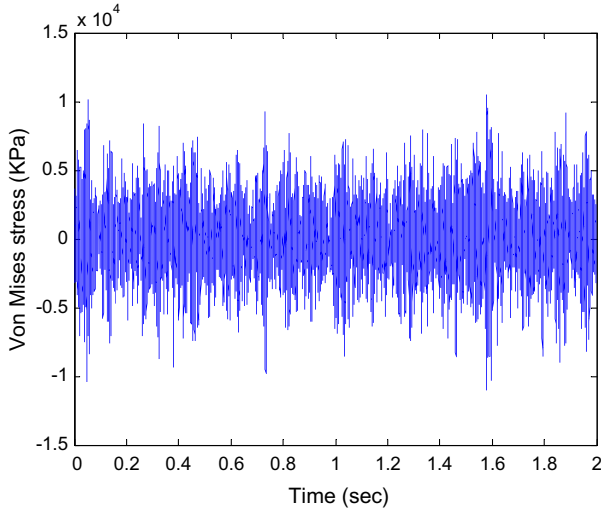


Fig. 14. Sample realization of time-history data generated from PSD.

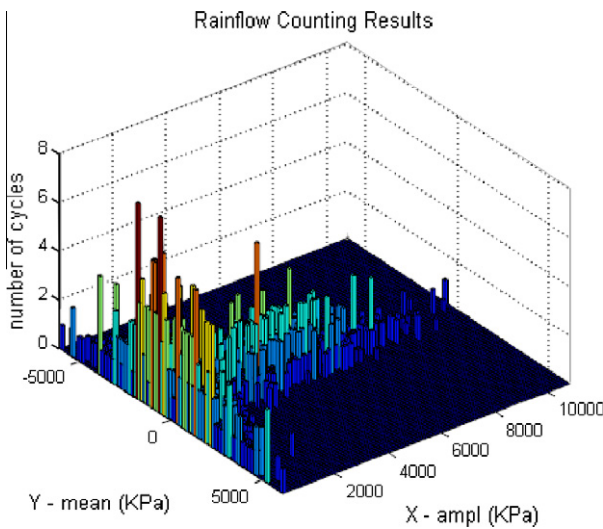


Fig. 15. Histogram of mean value and amplitude of the fatigue cycles obtained by the rainflow counting method.

where ΔS_i is the stress range of the cycle, S_{mi} is the mean stress of the cycle, S_u is the ultimate strength of the material, and b and c are constants obtained from the $S-N$ curve. ΔS_i and S_{mi} were obtained from rainflow counting results (Fig. 15). This procedure is especially helpful in properly accounting for the effect of mean stress, which could be very important in high-cycle fatigue analysis.

The cumulative damage index (CDI) is then written as

$$CDI = \sum_{i=1}^n \Delta D_i \tag{12}$$

It is assumed that failure occurs when the CDI equals a certain constant [1,25]. In this work, this constant is assumed to be 1.

The random vibration test results are summarized in Table 4 and Fig. 16. The results indicate a good fatigue life prediction of the solder joint especially for SAC405, it could be because SAC405 has a better $S-N$ curve fitting than SAC305 (SAC405's R^2 : 0.972, SAC305's R^2 : 0.768). Since the $S-N$ curve greatly affects the predicted fatigue life, more harmonic vibration tests need to be conducted to improve the curve fitting of SAC305 in future works.

Table 4

Comparison of time to failure results as obtained from FEA and random vibration tests.

Amplitude (g^2/Hz)	Frequency (Hz)	Average time to failure (min)	Predicted time to failure (min)	Difference (%)
0.25 (SAC305)	40–1000	113	121	+7.1
0.15 (SAC305)	40–1000	395	698	+76.7
0.25 (SAC405)	40–1000	102	93	-8.8
0.15 (SAC405)	40–1000	282	308	+9.2

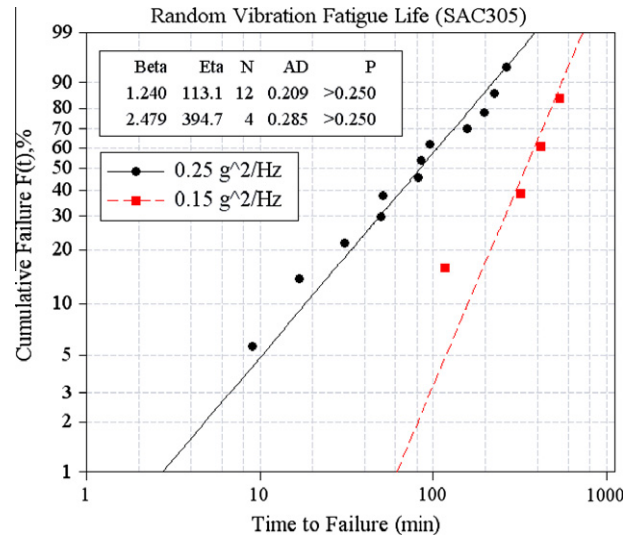


Fig. 16. Random vibration test results for SAC305.

4. Conclusion and discussion

This work is focused on predicting the fatigue life of electronic components under random vibration loading by combining both vibration tests and simulation analysis. To generate the $S-N$ curve, BGA package assemblies were tested under sinusoidal vibration loadings by varying the constant input G excitation. The time to failure was recorded during the sinusoidal vibration test and the number of cycle to failure was calculated. The FE model was built to obtain the resulting volume averaged Von Mises stress at critical solder joint. The $S-N$ curve was then determined with the stress from FEA and number of fatigue cycles from sinusoidal vibration tests.

Random vibration tests were conducted with white noise PSD of different acceleration amplitude as the input. The same FE model was applied to run the spectrum analysis in ANSYS to determine the response spectrum of the critical solder joint. The volume averaged PSD was calculated from the response PSD and then was used to simulate the time series data through IFFT. Rainflow cycle counting was applied to reduce a spectrum of varying stress into a set of simple stress reversals. Finally the Palmgren–Miner's rule was used to assess the fatigue life of BGA package.

The FE model was successfully validated by correlating with the natural frequencies, mode shapes and transmissibility function from the vibration tests. Also the FE model showed a good fatigue life prediction. Future work will study the effect of temperature on fatigue life.

Acknowledgments

This research work was partially supported by Samsung Electronics and IEEC of State University of New York at Binghamton. The authors appreciate the financial support.

References

- [1] Chen YS et al. Combining vibration test with finite element analysis for the fatigue life estimation of PBGA components. *Microelectron Reliab* 2008;48:638–44.
- [2] Che FX, Pang John HL. Vibration reliability test and finite element analysis for flip chip solder joints. *Microelectron Reliab* 2009;49:754–60.
- [3] Perkins A, Sitaraman SK. Vibration-induced solder joint fatigue failure of a ceramic column grid array (CCGA) package. In: Proc 54th electronic components and technology conference, Las Vegas; June 2004.
- [4] Yang QJ, Pang HLJ, Wang ZP, Lim GH, Yap FF, Lin RM. Vibration reliability characterization of PBGA assembly. *Microelectron Reliab* 2000;16:1097–107.
- [5] Pitarresi JM. Modeling of printed circuit cards subject to vibration. In: IEEE proceedings of the circuits and systems conference, New Orleans, LA; May 3–5, 1990. p. 2104–7.
- [6] Pitarresi JM et al. The smeared properties approach to FE vibration modeling of printed circuit cards. *ASME J Electron Pack* 1991;113(September):250–7.
- [7] Pitarresi JM, Akanda A. Random vibration response of a surface mounted lead/solder joint. In: Proc ASME international electronics packaging conference, vol. 1, Binghamton, NY; September 1993. p. 207–17.
- [8] Wong TE et al. Durability reliability of BGA solder joints under vibration environment. In: Proc 50th electronic components and technology conf; 2000. p. 1083–8.
- [9] Wu Mei-Ling. Vibration-induced fatigue life estimation of ball grid array packaging. *J Micromech Microeng* 2009;19(065005):12.
- [10] Li Ron S. A methodology for fatigue prediction of electronic components under random vibration load. *Trans ASME* 2001;123(December):394–400.
- [11] Zhou Y, Al-Bassyouni M, Dasgupta A. Harmonic and random vibration durability of SAC305 and Sn37Pb solder alloys. *IEEE Trans Compon Pack Technol* 2010;33(2). June.
- [12] Chin I, Wong SF, Malatkar P, Canham R. A mechanical fatigue assessment methodology to study solder joint reliability. In: 33rd international electronics manufacturing technology 1 conference; 2008.
- [13] Steinberg DS. *Vibration analysis for electronic equipment*. New York: Wiley; 1988.
- [14] Abdullah Al-Yafawi, Saket Patil, Da Yu, Seungbae Park, James Pitarresi. Random vibration test for electronic assemblies. In: Proc ITherm, Las Vegas; 2010.
- [15] IPC Test Standards, IPC-9701. Performance test methods and qualification requirements for surface mount solder attachments. IPC-association connecting electronics industries; 2002. p. 13.
- [16] Yang QJ, Wang ZP, Lim GH, John AA, Pang HL, Yap FF, et al. Reliability of PBGA assemblies under out-of-plane vibration excitation. *IEEE Trans Compon Pack Technol* 2002;25:293–300.
- [17] Miles RN. *Simulation of random fatigue life*. Suny-Binghamton; 2009.
- [18] Daewoong Suh et al. Effects of Ag content on fracture resistance of Sn–Ag–Cu lead-free solders under high-strain rate conditions. *Mater Sci Eng* 2007;595–603.
- [19] Pandher RS, Lewis BG, Vangaveti R, Singh B. Drop shock reliability of lead-free alloys-effect of micro-additives. In: Proc 57th electronic components and technology conf; 2007.
- [20] Jun Ming Hu. Sinusoidal vibration tests for product durability validation. European patent; 1997.
- [21] Steinberg DS. *Preventing thermal cycling and vibration failures in electronic equipment*. New York: Wiley; 2001.
- [22] Yao QZ, Qu JM, Wu SX. Solder fatigue life in two chip scale packages. In: Proc IEEE-IMAPS international symposium on microelectronics; 1999. p. 563–70.
- [23] Manson SS. Fatigue: a complex subject – some simple approximations. *Exp Mech* 1965;5:202–3.
- [24] Stephen Corda et al. In-flight vibration environment of the NASA F-15B flight test fixture, February 2002.
- [25] Wong SF, Malatkar P, Rick C, Kulkarni V, Chin I. Vibration testing and analysis of ball grid array package solder joints. In: Proc 57th electronic components and technology conference; 2007. p. 373–80.